

Preparation of M^0 metal/alumina-pillared mica composites (M=Cu, Ni) by *in situ* reduction of interlayer M^{2+} ions of alumina-pillared fluorine micas

Tomohiro Yamaguchi, Seiichi Taruta, Tomohiko Yamakami and Kunio Kitajima

Department of Chemistry and Material Engineering, Faculty of Engineering, Shinshu University,
4-17-1 Wakasato, Nagano-shi 380-8553, Japan

Abstract

Alumina-pillared fluorine micas form micropores in the interlayer region and exhibit cation exchangeability. Reduction of 3d transition metal cations (Cu^{2+} and Ni^{2+}) in the interlayer regions of the cation exchanged alumina-pillared micas was attempted using ethylene glycol or diethylene glycol. The Cu^{2+} -exchanged pillared mica led to the formation of a pillared mica composite containing interlayer zero-valence Cu^0 metal clusters along with Cu^0 metal fine particles on external surfaces of pillared mica flakes when refluxed in either ethylene glycol or diethylene glycol. Ni^{2+} cations in the interlayer region were also found to be reducible by refluxing in diethylene glycol. The zero-valence metal contained in the refluxed products occurs in three forms: M^0 clusters in the interlayer region, elongated fine particles sandwiched between silicate layers, and submicron spherical particles on external surfaces of mica crystals. The zero-valence metal/alumina-pillared mica composites thus obtained largely retained the micropore properties of the alumina-pillared micas.

KEYWORDS:

A. layer compounds, A. microporous materials, B. intercalation reactions, C. electron microscopy, C. X-ray diffraction

1. Introduction

Intercalation of bulky inorganic polycations into the interlayer region of swelling clays by cation exchange and subsequent heat treatment produces thermally stable microporous solids, namely, pillared clays. In pillared clays, the intercalated and immobilized oxides formed upon heating prop the layers apart as pillars. Pillared clays exhibit interesting properties for catalysis, adsorption and separation. Synthetic swellable fluorine micas [1,2] can be used as host crystals for intercalation [3,4]. These synthetic micas are characterized by large cation exchange capacity, high crystallinity and high thermal durability. Pillared fluorine micas are obtainable in the same manner by using natural clays as host crystals [5-8].

Pillared clays have two-dimensional pores in the interlayer region between pillars, while zeolites have three-dimensional pores in the crystal structure. In general, the pore size of pillared clays is larger than that of zeolites and smaller than that of inorganic meso- and macroporous solids such as silica and alumina [9,10]. The pore size and physicochemical properties of pillared clays can be controlled by varying both the host crystals and pillaring agents. Recently, we reported the synthesis and properties of alumina-pillared fluorine micas having high cation exchangeability resulting from the high content of residual interlayer Na^+ along with its fixation behavior upon heating [11]. The unique cation exchangeability of the pillared micas is expected to enable chemical modification of their properties and extend their applicability into a wider variety of fields.

In situ reduction of interlayer cations such as Cu^{2+} , Ag^+ , Pd^{2+} or Pt^{2+} in montmorillonite by a polyol process [12] using ethylene glycol has been reported [13-16]. Furthermore, we reported that reduction of interlayer Co^{2+} ions in swellable fluorine mica could be accomplished by using diethylene glycol [17]. These polyol reduction processes are expected to be applicable to cation exchanged alumina-pillared fluorine micas for obtaining composites or nanocomposites having a high dispersion of metal particles in a matrix of alumina-pillared fluorine micas. The cation

exchange of M^{2+} ions results in more intimate and homogeneous mixing with the matrix of the pillared mica than the ordinary impregnation process using salt solutions for pillared clays prepared from natural clay minerals. Sinterability of alumina-pillared mica powders at low temperatures [6-8] is also promising from the standpoint of obtaining bulky sintered composites. Against this background, we attempted to reduce 3d transition metal cations (Cu^{2+} and Ni^{2+}) in the interlayer regions of cation exchanged alumina-pillared micas using polyols, such as ethylene glycol and diethylene glycol, as reducing agents. The aims of this paper are to determine (i) whether interlayer Cu^{2+} and Ni^{2+} ions are reducible, and (ii) the distribution of corresponding metal clusters or fine particles in the matrix of refluxed products.

2. Experimental

Na-tetrasilicic fluorine mica (Na-TSM), $NaMg_{2.5}Si_4O_{10}F_2$, was used as host crystal for the preparation of pillared mica [5-8,11]. Na-TSM was synthesized by a procedure described previously [1,11]: reagent-grade NaF, MgF_2 , MgO and SiO_2 were used as raw materials; these were mixed in a proportion corresponding to the stoichiometry of Na-TSM, sealed in a platinum tube and then melted in an electric furnace at $1450^\circ C$ for 2 h. The polyhydroxoaluminum (PHA) solution used as pillaring agent was prepared by the Al metal dissolving method [18]. The solution had an OH/Al ratio of 2.50 and an Al concentration of 6.05 mol/dm^3 . A suspension containing mica crystals was allowed to react with the diluted PHA solution at $65^\circ C$ for 24 h under vigorous stirring with a solution loading of $44.8 \text{ mmol (Al)/1.0 g-mica}$. The product was washed several times, dried at $65^\circ C$ and then calcined at $500^\circ C$ for 2 h to obtain alumina-pillared mica (APM).

APM powders were reacted with a 0.1 mol/l $CuSO_4$ or $NiSO_4$ solution. The ion exchanged APMs (M^{2+} -APM, where $M = Cu$ or Ni) were washed thoroughly with distilled water to remove excess salts. The M^{2+} -APMs were suspended in ethylene glycol (EG) or diethylene glycol (DEG) and refluxed in nitrogen atmosphere for 90 min. After the reaction, the refluxed products (M-EG-APM or

M-DEG-APM) were washed with ethanol and dried in air at room temperature. A portion of the M-EG-APM and M-DEG-APM was heated at 400°C in an inert atmosphere to remove interlayer residual polyol molecules. The products were characterized by X-ray diffraction (XRD), scanning electron microscopy (SEM) and transmission electron microscopy (TEM), and N₂ adsorption-desorption measurements.

3. Results and discussion

Fig. 1 shows the XRD pattern of the APM sample. The sharp (001) profile of the pillared mica appeared at around 4.9° (CuK α), indicating that a pillared structure with a basal spacing of 1.77 nm was formed. In addition, the pillared mica gave rational high-order (00*l*) reflections, showing regular interstratification. PHA cations as a pillar precursor are converted into alumina pillars in the interlayer regions at 300-500°C [19] so that dehydration and dehydroxylation of the pillar precursor to form rigid pillars were completed for the APM sample at 500°C. Furthermore, our previous study on the cation exchange of alumina-pillared fluorine micas showed that the amount of exchanged cation reached a maximum upon heat-treatment at 500°C owing to the counterbalance between freed and fixed Na⁺ ions [11]. Thus, the APM sample used for refluxing exchanged ca. 30 mEq/(100 g pillared mica) of the Ni²⁺ cation.

The isotherm of APM was of type I according to IUPAC classification, and its BET specific surface area calculated from the isotherm was 208 m²/g. SEM revealed a flaky morphology based on a layer stacking structure. The maximum dimensions parallel and perpendicular to the layers were about 30 μ m and 2 μ m, respectively, showing that the APM flakes are much larger than those of natural clays.

Fig. 2 shows XRD patterns of the refluxed products. Each product gave a sharp (001) reflection at the same diffraction angle for the APM sample before refluxing. XRD pattern of Cu-EG-APM showed trace diffraction lines ascribable to Cu⁰ metal. Cu-EG-APM and Ni-DEG-APM exhibited a metallic color, a

reddish and grayish color, respectively, while the Ni-EG-APM sample retained its pale green color. Cu-DEG-APM also showed a reddish color. These findings indicate that the Cu^{2+} ions in the interlayer region of the pillared mica were reduced into Cu^0 metal by refluxing in either EG or DEG, while the Ni^{2+} ions were reduced into Ni^0 only when refluxed in DEG. The difference in reducibility of Cu^{2+} and Ni^{2+} ions in the interlayer regions of the pillared mica resulted from the difference in oxidation-reduction potential. Indeed, the present authors have reported that interlayer Co^{2+} ions, which have a higher oxidation-reduction potential than Cu^{2+} and Ni^{2+} ions, could only be reduced when refluxed in DEG [17]. Hinotsu et al. [20] reported the preparation of Ni^0 nanoparticles by the polyol process using nickel acetate tetrahydrate as metal precursor and ethylene glycol as polyol. Li et al. [21] also reported the preparation of Ni^0 nanoparticles from nickel acetate tetrahydrate through a microwave-assisted polyol process using ethylene glycol. These studies suggest the feasibility of reducing interlayer Ni^{2+} ions in pillared mica using ethylene glycol, however, this was found to be difficult under the present conditions.

When Cu^{2+} -APM is refluxed in EG or DEG, the *in situ* reduction of Cu^{2+} that occurs in the interlayer regions of APM decreases the overall positive charge of the interlayer materials. However, this positive charge deficiency is compensated by the introduction of protons derived from polyol molecules during the polyol-oxidation reaction, as in the case of the reduction of Co^{2+} in fluorine mica [17]. Thus, owing to the decrease in positive charge, part of the reduced Cu metal is likely to migrate from the interlayer to the outer surface of mica flakes to form fine Cu^0 particles.

Fig. 3 shows SEM micrographs of the refluxed products after heating at 400°C in an inert atmosphere to eliminate residual intercalated organic molecules. Spherical particles were observed on external surfaces, especially at vertical surfaces of or kinks in the pillared mica flakes, as seen in Figs. 3a and 3c. These particles were identified as Cu^0 and Ni^0 metal, respectively, by energy-dispersive X-ray analysis. The sizes of the deposited fine metal particles were less than $0.5\ \mu\text{m}$ for Cu-EG-APM,

Cu-DEG-APM and Ni-DEG-APM. No deposited Ni⁰ metal particles were detected in the Ni-EG-APM sample, as seen in Fig. 3b.

A possible reaction mechanism for reducing transition metal cations using EG by a polyol process was described by Fievet et al. [12]. The reduction in the present case presumably occurs through a mechanism similar to that observed in the case of swellable clay minerals because the M²⁺ ions in APM are located in the interlayer region as exchangeable cations and compensate the negative charge of the silicate layers. The loss of positive charge during the reduction reaction $M^{2+} \rightarrow M^0$ frees M⁰ clusters from the electrostatic interaction with the negatively charged silicate layers and induces the M⁰ clusters to migrate from the interlayer region onto the external surface of the pillared mica flakes. Although the charge transfer mechanism through the interaction of metal clusters with surface oxygens [14,15] may be effective for stabilization of metal clusters in the interlayers, reduced metal particles, ranging in size from 0.2 to 0.5 μm, on the external surfaces of silicate flakes were also reported for the reduction of Cu²⁺ in montmorillonite [13-15] and Co²⁺ in swellable fluorine mica [17]. Nevertheless, at least in the initial stage of reduction, some of the reduced metal (Cu⁰ and Ni⁰) clusters will be enclosed in the interlayer region of APM, modifying the interlayer nano-space.

TEM micrographs of the Cu-EG-APM sample are shown in Fig. 4. The sample was embedded in resin, cut and then ion-milled before TEM observation. Elongated oval particles, as distinct from the spherical particles on the external surface shown in Fig. 3, were observed inside the APM interstratifications with their long axes oriented parallel to the silicate layers (Fig. 4a). The oval particles were located between the silicate layers, which were forced to curve around the particles, and their long axis dimension was less than about 200 nm. However, much finer particles or clusters were observed as well (Fig. 4b). These findings indicate that the reduced Cu²⁺ ions form Cu⁰ metal clusters in the two-dimensional interlayer space during the initial stage of the reaction, and these clusters then grow into elongated particles as a

result of two-dimensional diffusion along the silicate layers. Some of the elongated fine particles may migrate to reach the outer surfaces of APM and grow further into larger spherical particles. The distribution of clusters, elongated fine particles and larger external particles depends on the kinetics of the reaction, the lateral dimension of the mica flakes and the types of defects in the mica layer-stacking structure, i.e., the low-angle tilt boundary.

Table 1 lists the basal spacings and some pore properties of the products. All the refluxed products had a basal spacing of 1.8 nm, which is the same as that of the APM sample, indicating that the products retained their pillared structure. On the other hand, the BET surface area, micropore volume and total pore volume of the refluxed products decreased in relation to those of the APM sample. This presumably indicates that the metal clusters that formed during the polyol process occupy part of the interlayer nano-space. This is supported, in particular, by the fact that the micropore area and micropore volume of M-EG (or DEG)-APMs were decreased; for example, Cu-EG-APM showed a micropore area of 125 m²/g and micropore volume of 0.08 cm³/g, while the corresponding values for APM were 159 m²/g and 0.10 cm³/g. The decrease in BET surface area and pore volume may also be caused by the residues of thermal decomposition products formed from intercalated polyol molecules. Despite the slight decrease in surface area and pore volume, the refluxed products, i.e., the M⁰ metal/alumina-pillared mica composites, still exhibited micropores in their interlayers, which demonstrates that the reduction of M²⁺-exchanged pillared micas provides a new route for obtaining unique M⁰-doped nanocomposites.

4. Conclusions

In situ reduction of 3d transition metal cations (Cu²⁺ and Ni²⁺) in the interlayer regions of cation exchanged microporous alumina-pillared micas was attempted using polyols as reducing agents. Refluxing the Cu²⁺-exchanged pillared mica in either ethylene glycol or diethylene glycol led to reduction of Cu²⁺ cations into Cu metal (Cu⁰) clusters in the interlayer of the pillared mica.

Ni²⁺ cations in the interlayer of the pillared mica were also reducible by refluxing in diethylene glycol but not in ethylene glycol. The interlayer Cu⁰ clusters tended to coalesce into elongated oval particles between the curved silicate layers. The long-axis dimension of these elongated oval particles was less than about 200 nm. Furthermore, submicron spherical metal particles were deposited on external surfaces of the host mica crystals. The M⁰-doped composites thus obtained retained the microporous properties of the mother pillared micas and showed a BET specific surface area of ca. 180 m²/g.

Acknowledgement

This work was supported by a Grant-in-Aid for Young Scientists (B) (16750169) from the Ministry of Education, Culture, Sports, Science and Technology (MEXT) of Japan.

References

- [1] K. Kitajima, N. Daimon, *Nippon Kagaku Kaishi* (6) (1975) 991.
- [2] K. Kitajima, F. Koyama, N. Takusagawa, *Bull. Chem. Soc. Jpn.* 58 (4) (1985) 1325.
- [3] M. Ogawa, M. Hama, K. Kuroda, *Clay Miner.*, 34 (1999) 213.
- [4] T. Sivakumar, T. Krithiga, K. Shanthi, T. Mori, J. Kubo, Y. Morikawa, *J. Mol. Catal. A-Chem.* 223 (2004) 185.
- [5] K. Ohtsuka, Y. Hayashi, M. Suda, *Chem. Mater.* 5 (12) (1993) 1823.
- [6] T. Yamaguchi, Y. Sakai, K. Kitajima, *J. Mater. Sci.* 34 (1999) 5771.
- [7] T. Yamaguchi, A. Shirai, S. Taruta, K. Kitajima, *Ceram.-Silik.* 45 (2) (2001) 43.
- [8] T. Yamaguchi, T. Ito, Y. Yajima, S. Taruta, K. Kitajima, *J. Ceram. Soc. Japan, Suppl.* 112 (5) (2004) S21.
- [9] C.T. Kresge, M.E. Leonowicz, W.J. Roth, J.C. Vartuli, J.S. Beck, *Nature* 359 (1992) 710.
- [10] S.A. Bagshaw, T.J. Pinnavaia, *Angew. Chem. Int. Ed. Engl.* 35 (10) (1996) 1102.
- [11] T. Yamaguchi, K. Kitajima, E. Sakai, M. Daimon, *Clay*

- Miner., 38 (2003) 41.
- [12] F. Fievet, J.P. Lagier, B. Blin, B. Beaudoin, M. Figlarz, *Solid State Ionics* 32/33 (1989) 198.
- [13] P. Ravindranathan, P.B. Malla, S. Komarneni, R. Roy, *Catal. Lett.* 6 (1990) 401.
- [14] P.B. Malla, P. Ravindranathan, S. Komarneni, R. Roy, *Nature* 351 (1991) 555.
- [15] P.B. Malla, P. Ravindranathan, S. Komarneni, E. Breval, R. Roy, *J. Mater. Chem.* 2 (5) (1992) 559.
- [16] S. Komarneni, M.Z. Hussein, C. Liu, E. Breval, P.B. Malla, *Eur. J. Solid State Inorg. Chem.* 32 (1995) 837.
- [17] T. Yamaguchi, K. Kitajima, *J. Mater. Sci.* 33 (1998) 653.
- [18] T. Fujita, K. Kitajima, S. Taruta, N. Takusagawa, *Nippon Kagaku Kaishi* (4) (1993) 319.
- [19] P. Cool, E.F. Vansant, in: H.G. Karge, J. Weitkamp (Eds), *Molecular Sieves vol.1*, Springer, 1998, pp. 265-288 (ISBN 3-540-63622-6).
- [20] T. Hinotsu, B. Jeyadevan, C.N. Chinnasamy, K. Shinoda, K. Tohji, *J. Appl. Phys.* 95 (11) (2004) 7477.
- [21] D. Li, S. Komarneni, *J. Am. Ceram. Soc.* 89 (5) (2006) 1510.

Figure captions

Fig. 1. XRD pattern of the Al_2O_3 -pillared fluorine mica.

Fig. 2. XRD patterns of the refluxed products.

(a) Cu-EG-APM, (b) Ni-EG-APM and (c) Ni-DEG-APM.

Fig. 3. SEM micrographs of the refluxed products.

(a) Cu-EG-APM, (b) Ni-EG-APM and (c) Ni-DEG-APM.

Fig. 4. TEM micrographs of the Cu-EG-APM sample.

Table 1. Properties of M⁰/ Al₂O₃-pillared micas.

Sample	Basal spacing /nm	BET specific surface area /m ² g ⁻¹	Micropore volume /cm ³ g ⁻¹	Total pore volume /cm ³ g ⁻¹
Al ₂ O ₃ -pillared mica	1.77	208	0.104	0.130
Cu ⁰ / Al ₂ O ₃ -pillared mica (Cu-EG-APM)	1.77	172	0.080	0.127
Ni ⁰ / Al ₂ O ₃ -pillared mica (Ni-DEG-APM)	1.77	181	0.083	0.122

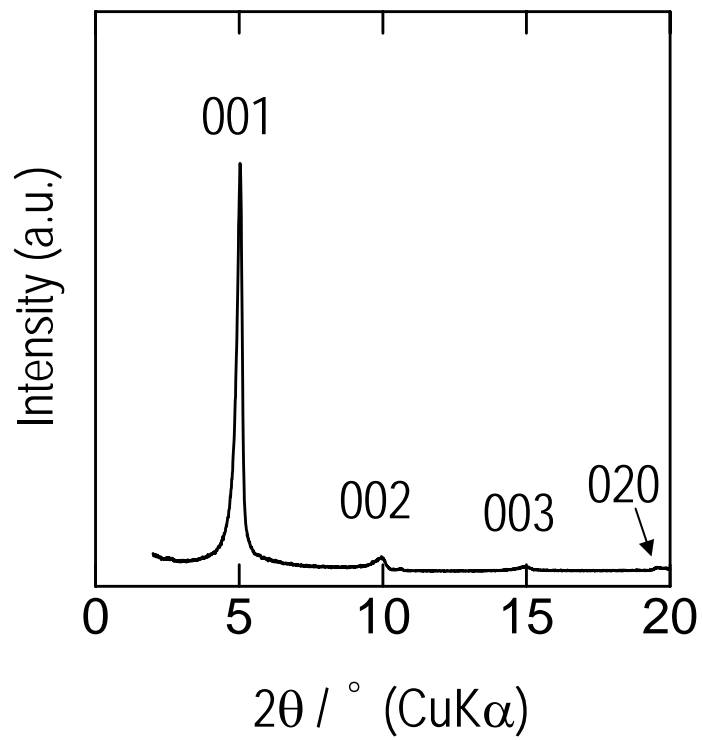


Fig. 1

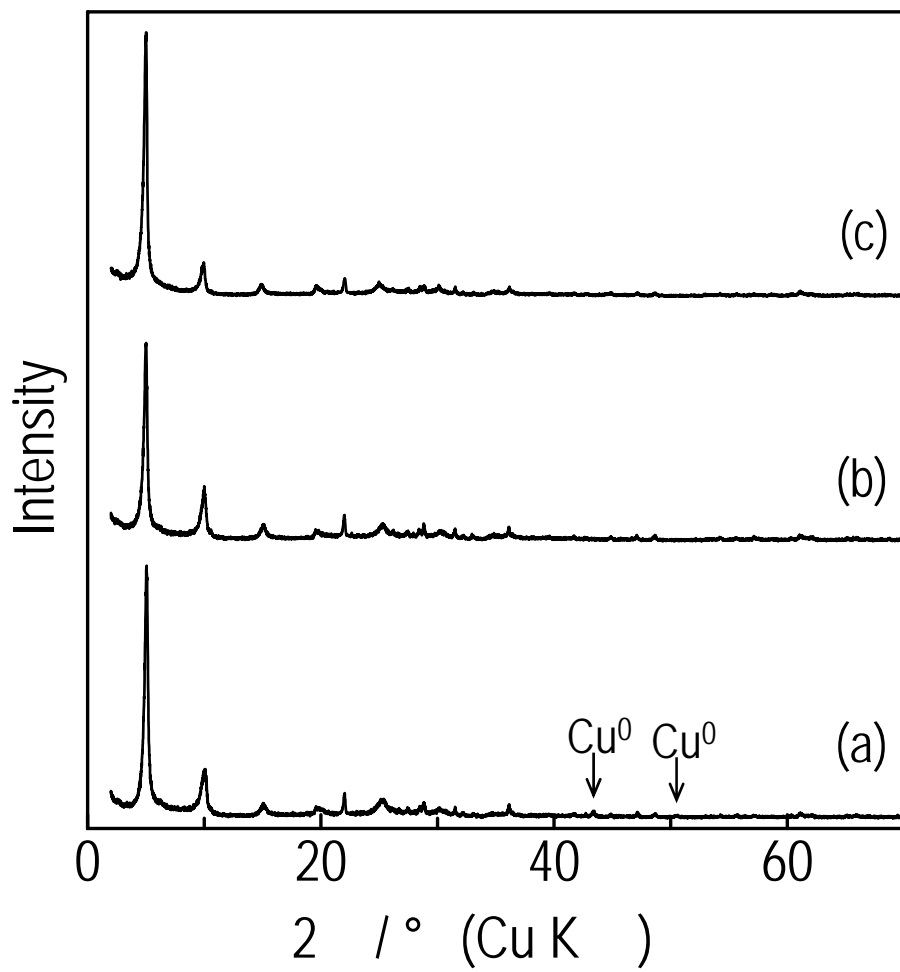


Fig. 2

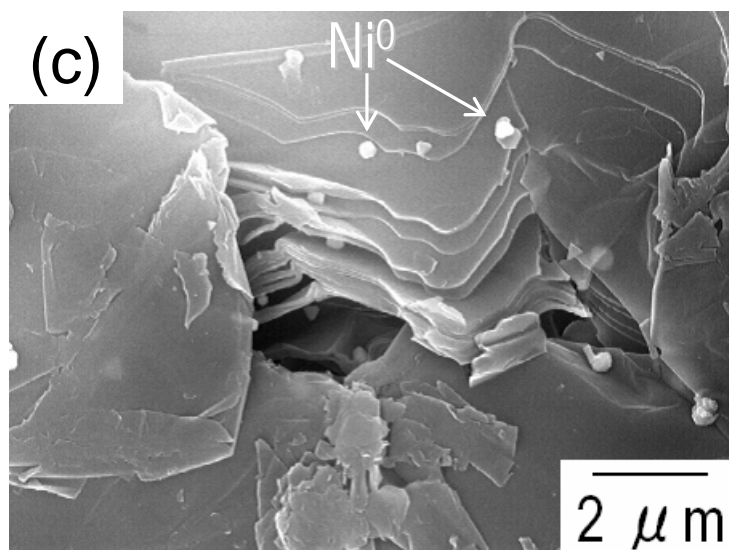
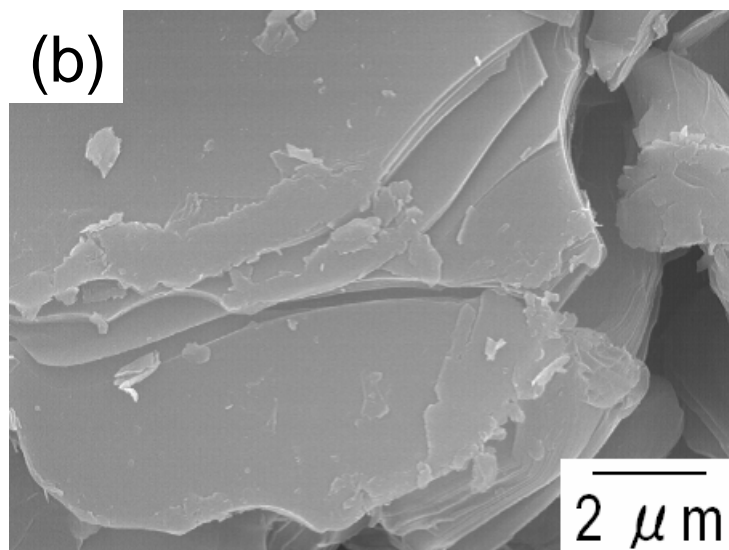
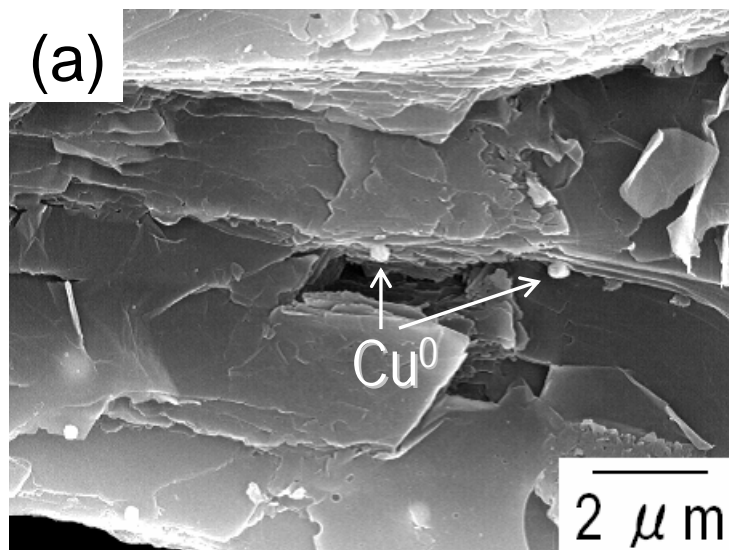


Fig. 3

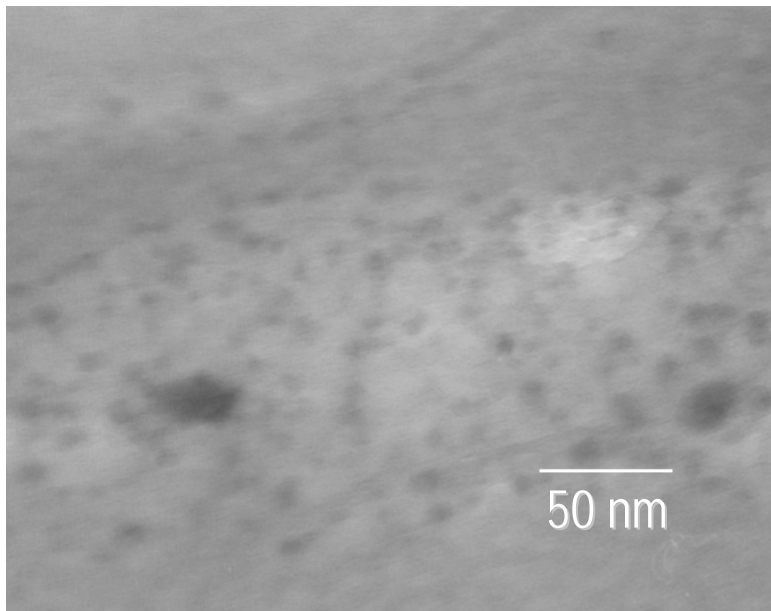
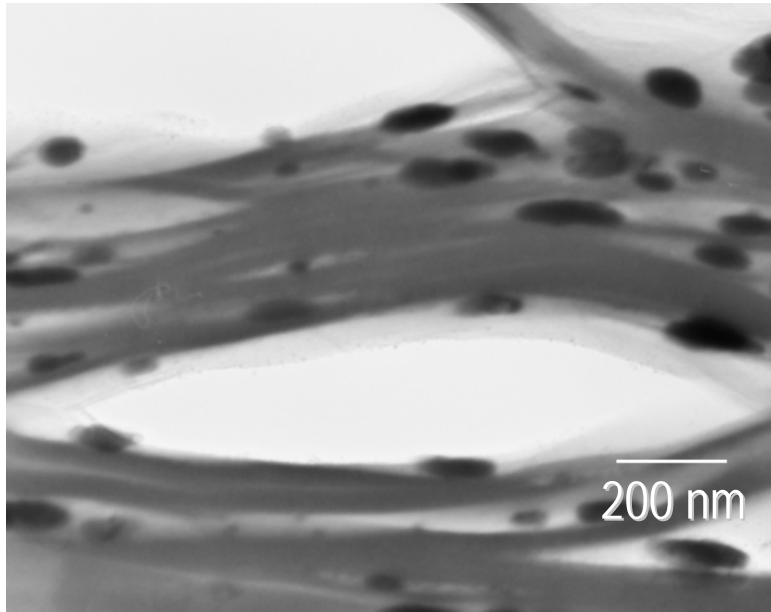


Fig. 4